

## Nanobelts as nanocantilevers

William L. Hughes and Zhong L. Wang<sup>a)</sup>

*School of Materials Science and Engineering, Georgia Institute of Technology, Atlanta, Georgia 30332-0245*

(Received 3 January 2003; accepted 7 March 2003)

Semiconducting oxide nanobelts of ZnO have been sectioned and manipulated, for microelectromechanical systems, using an atomic force microscopy probe. Structurally modified nanobelts demonstrate potential for nanocantilever based technologies. With dimensions  $\sim 35$ –1800 times smaller than conventional cantilevers, the nanocantilevers are expected to have improved physical, chemical, and biological sensitivity for scanning probe microscopy and sensor applications. © 2003 American Institute of Physics. [DOI: 10.1063/1.1570497]

Cantilever based scanning probe microscopy (SPM) techniques are among the most powerful approaches for imaging, manipulating and measuring nanoscaled properties and phenomena. SPMs generate images by measuring forces between sample surfaces and microscope probes. Common forces detected using SPMs are the van der Waals force, electrostatic force, capillary force, and double-layer force.<sup>1</sup> Conventional SPM cantilevers are fabricated from silicon, SiC and Si<sub>3</sub>N<sub>4</sub> using electron-beam or optical lithography. A typical SPM cantilever has a length, width, and thickness of  $\sim 125$ ,  $\sim 35$ , and  $\sim 4$   $\mu\text{m}$ , respectively. The resolution of a SPM is limited by three factors: (1) the shape of the tip, (2) the sample-tip contact, and (3) the ability to measure the sample-tip interaction.

Ideally an SPM probe would be a robust one-dimensional structure, while the cantilever would pose ultrahigh sensitivity to any and all forces. Currently, Dai *et al.* have developed atomic force microscope tips by growing carbon nanotubes on the ends of standard atomic force microscopy (AFM) probes.<sup>2–4</sup> These high aspect ratio tips are nearly ideal for AFM imaging because of their size and durability. As a result, the nanotubes can image surfaces with a large degree of abrupt variation in surface morphology. Also, Rugar *et al.* are developing geometrically small single crystal silicon cantilevers in an attempt to measure the electronic spin of materials.<sup>5</sup> The relevant technologies listed earlier are examples of the need for decreased cantilever size in SPM applications. The capabilities of nanotube tips will not be fully exploited until the cantilever is sensitive to all nanotube-surface interactions; nor can imaging of electronic spin occur until measurements of forces in the sub-atonewton range become a reality. Utilization of nanowire based cantilevers offer a potential solution to the aforementioned problems.<sup>6,7</sup>

Recently, long ribbon-like nanostructures of semiconducting oxides and sulfides, such as, CdO, ZnO, Ga<sub>2</sub>O<sub>3</sub>, PbO<sub>2</sub>, In<sub>2</sub>O<sub>3</sub>, SnO<sub>2</sub>, and ZnS have been synthesized within our laboratory.<sup>8,9</sup> Nanobelt size and geometry are controlled during solid-state thermal evaporation processes without the aid of a catalyst. Figure 1(a) shows a CdO nanobelt that has been bent without fracture, indicating mechanical flexibility and toughness. The CdO nanobelts grow along [100] or

[010] directions, and can form zig-zag shapes by switching the growth direction [Fig. 1(b)]. Nanobelts range between 50 nm and 1  $\mu\text{m}$  in length, 20 nm and 1  $\mu\text{m}$  in width, and width to thickness ratios of  $\sim 9$ .<sup>8</sup> Nanobelts are single crystals with specific oriented surfaces. The rectangular cross section, uniform thickness, and ribbon (belt)-like morphology make nanobelts an ideal candidate for cantilever applications. Geometrically, nanobelts are significantly smaller than current cantilever technology and thus more sensitive to all detectable forces.

Nanobelts differ from conventional nanowires by being nearly void of dislocations and other line defects. A reduc-

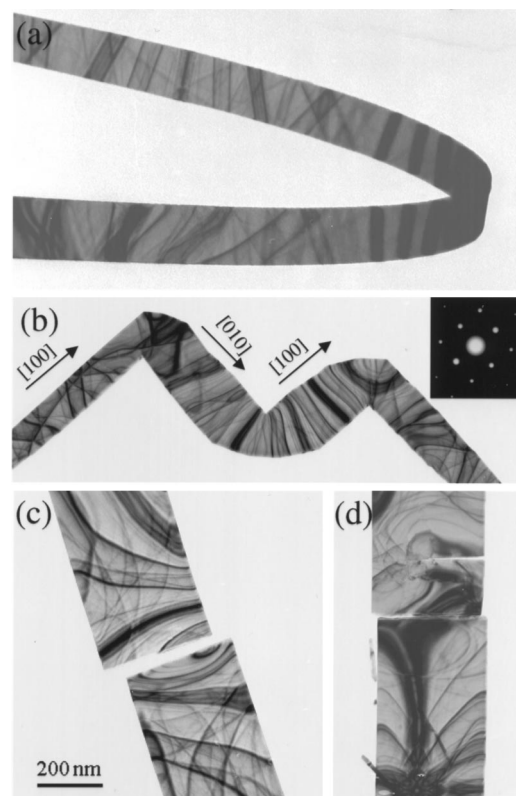


FIG. 1. (a), (b) TEM images of CdO nanobelts, showing the flexibility and toughness of the nanobelt. The electron diffraction inset in (b) illustrates the single crystalline structure of the nanobelt. (c), (d) Cutting a CdO nanobelt by an electron beam in TEM. This operation uses the ionic structure of CdO, thus, a small force results in the displacement of the lattice, leading to crystal cleavage.

<sup>a)</sup>Electronic mail: zhong.wang@mse.gatech.edu

tion in line defects increases the electronic and optoelectronic performance of a material. Also, nanobelts are wide band gap semiconductors, which are made from transparent conducting oxides for applications in optics, sensors, and functionalized surface coatings. Using the intrinsic semiconducting property of nanobelts, field effect transistors have been fabricated using individual nanobelts and demonstrated to exhibit interesting optoelectronic properties.<sup>10</sup> Gas sensors have also been fabricated using single crystalline SnO<sub>2</sub> nanobelts. Electrical characterization showed that the contacts were ohmic and the nanobelts were sensitive to environmental polluting species like CO and NO<sub>2</sub> as well as ethanol for breath analyzers and food control applications.<sup>11</sup> The results demonstrate the potential of fabricating nanosize sensors using the integrity of a single nanobelt with sensitivity at the level of a few parts per billion.

Manipulation of nanobelts is vital to the development and fabrication of nanoscale functional devices. In this letter, we will illustrate manipulation of ZnO nanobelts via transmission electron microscopy (TEM) and AFM. ZnO nanobelts have been sectioned at specified locations into various lengths using an atomic force probe. Exploiting the nearly ideal morphology of nanobelts, we will elaborate on manipulation techniques required to form nanocantilevers. Nanobelt cantilevers are  $\sim 35$ –1800 times smaller than conventional cantilevers. Sawing, fracturing, and lifting ZnO nanobelts will be presented as a means for cantilever fabrication.

Integration of structurally controlled nanomaterials with microelectronic mechanical systems (MEMS) requires precise manipulation. The first task is to cut nanobelts into specific lengths. We have previously shown the ability to cleave CdO nanobelts by a focused electron beam in a JEOL 100C transmission electron microscope [Figs. 1(c) and 1(d)].<sup>8</sup> In this letter, two additional techniques have been used to section nanobelts. One method is to effectively saw through the nanobelt by: (1) increasing the aspect ratio of the viewing screen during AFM operation, (2) minimizing the scan size to capture only the width of a nanobelt, and (3) increasing the integral and proportional gains and thus increasing the applied force on the nanobelt during scanning. This technique can be used in either tapping mode or contact mode. Problems with this method are its laborious nature and difficulty in quantifying nanobelt degradation with increasing time. The second method increases the force applied to the nanobelt while engaged in force calibration mode of the SPM. This technique fractures nanobelts by driving the AFM silicon probe into their surface and is extremely reproducible.

Images for two independent ZnO nanobelts that were sawed and fractured are shown later in Figs. 2(a) and 2(b) and Figs. 2(c) and 2(d), respectively. The numbered circles, within the images, correspond to multiple cutting attempts and increase with increasing cuts. It should be noted; image quality for atomic force microscopes is directly related to the tip-surface interaction.<sup>12</sup> Since the atomic force probe was used as a cutting device, with high contact forces, the image quality degraded with increasing time. This observation is common during prolonged tip use or fracture.<sup>12</sup> However, the intentions of this experiment were not to develop high quality AFM images, but to show the ability of an AFM to section

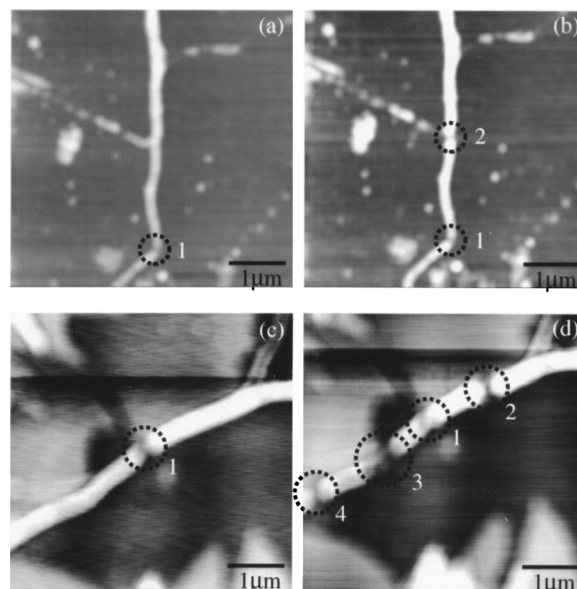


FIG. 2. (a), (b) AFM image of a ZnO nanobelt that has been sawed. (c),(d) AFM image of a ZnO nanobelt that has been fractured. Images were captured using a Dimension 3000 SPM in tapping mode operation.

nanobelts into specified lengths for cantilever applications. Fracturing of nanobelts is possible because the bond character is primarily ionic in nature, and thus an atomic displacement of half the lattice constant generates a cleavage due to Coulomb repulsion.

Tip contamination is a common annoyance in microscopy. However, when controlled, tip contamination becomes a critical tool for selectively picking up nanostructures and moving them from one substrate to another. Using a Dimension 3000 SPM in tapping mode, we have successfully lifted ZnO nanobelts from a silicon substrate. Capillary forces are responsible for the adhesion strength between the atomic force microscope probe and the ZnO nanobelts. An example of tip contamination is shown later in Fig. 3. It should be noted that Fig. 3 is a real-time optical image gathered from a Dimension 3000 optical monitor. The image exemplifies the ability of an atomic force microscope to selectively pickup individual nanobelts.

Combining the aforementioned techniques with micro-

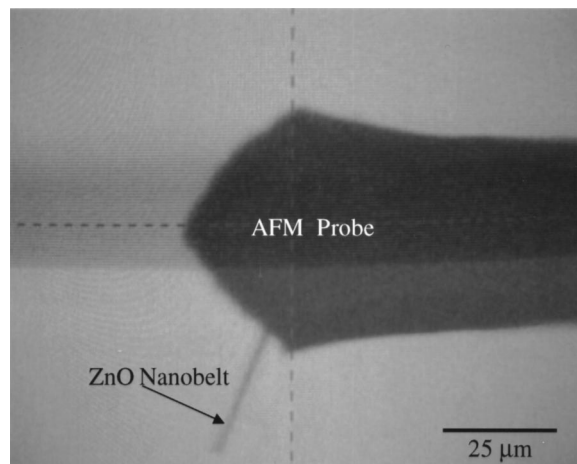


FIG. 3. Optical image of a ZnO nanobelt attached to an AFM probe as a nanocantilever.

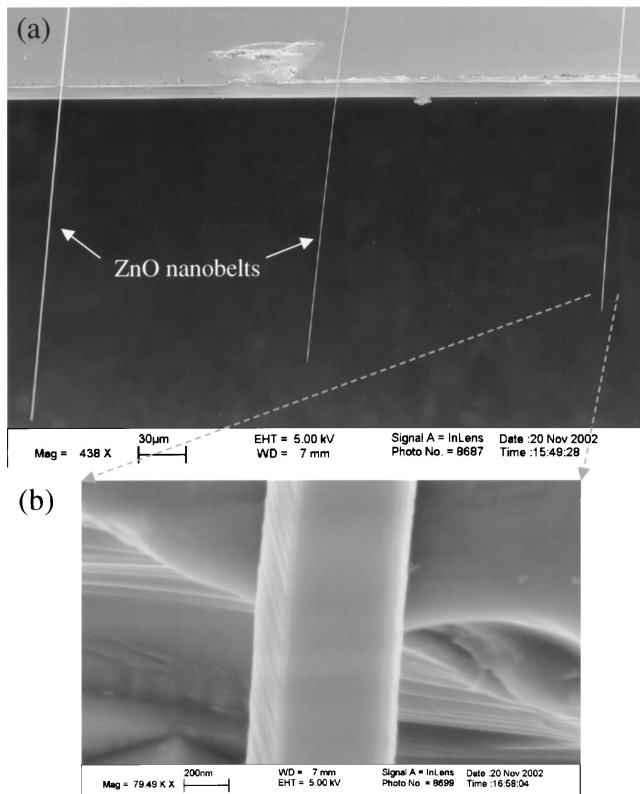


FIG. 4. (a) Site specific placement and alignment of ZnO nanobelts onto a silicon chip, forming nanocantilever arrays. (b) An enlarged scanning electron microscopy image of the third nanocantilever showing its shape; the width of the cantilever was measured to be 525 nm. SEM was carried out using a LEO 1530 FEG SEM.

manipulation has led to the horizontal alignment of individual ZnO nanobelts onto silicon chips. The aligned ZnO cantilevers, shown in Fig. 4, were manipulated to have a range of lengths. This exemplifies our ability to tune the resonance frequency of each cantilever and thus modify cantilevers for different applications such as contact, noncontact, and tapping mode AFM. Periodic contrast of the ZnO cantilevers is observed as a result of electronic charge induced vibrations during SEM operation. Such contrast is absent in regions where the nanobelts are in direct contact with the silicon substrate, suggesting adequate adhesion forces between the cantilevers and the silicon chip.

Combining MEMS technology with self-assembled nanobelts we are able to produce cost effective cantilevers with heightened sensitivity for a range of devices and applications. Force, pressure, mass, thermal, biological, and chemical sensors are all prospective devices.<sup>13–15</sup> Semicon-

ducting nanobelts are ideal candidates for cantilever applications. Structurally they are defect free single crystals, providing excellent mechanical properties. The elastic modulus for a ZnO nanobelt has been measured by an *in situ* TEM technique based on electromechanical resonance.<sup>16</sup> Geometrically, the rectangular cross section of nanobelts provides two distinctive resonant frequencies, corresponding to two orthogonal vibration directions.<sup>16</sup> These opposing resonant frequencies can be exploited as alternative detection modes for many cantilever applications. Finally, the reduced dimensions of nanobelt cantilevers offer a significant increase in cantilever sensitivity.<sup>12</sup>

Although preliminary in nature, the work demonstrated in this letter is critical to the development of next generation physical, chemical, and biological sensors and probes based on cantilever technology. The ability to dimensionally control and manipulate nanobelts for cantilever devices and applications establishes a framework from which ultra sensitive cantilevers will be developed.<sup>17</sup>

Research supported by the NASA URETI program and Georgia Tech. The Dimension 3000 SPM was a loan from the Monsanto Company. Thanks to Dr. Jingyue Liu for stimulating discussions. Thanks to Dr. Z. W. Pan for sharing Fig. 1.

- <sup>1</sup>H. J. Guntherodt, D. Anselmetti, and E. Meyer, *Forces in Scanning Probe Method* (Kluwer Academic, Netherlands, 1995).
- <sup>2</sup>H. Dai, E. Yenilmez, Q. Wang, R. J. Chen, and D. Wang, *Appl. Phys. Lett.* **80**, 12 (2002).
- <sup>3</sup>H. Dai, W. Kim, Y. Zhang, M. Rolandi, and D. Wang, *J. Phys. Chem. B* **105**, 11424 (2001).
- <sup>4</sup>H. Dai, N. R. Franklin, Y. Li, R. J. Chen, and A. Javey, *Appl. Phys. Lett.* **79**, 27 (2001).
- <sup>5</sup>D. Rugar, T. D. Stowe, K. Yasumura, T. W. Kenny, D. Botkin, and K. Wago, *Appl. Phys. Lett.* **71**, 2 (1997).
- <sup>6</sup>P. Yang and C. M. Lieber, *Science* **273**, 1836 (1996).
- <sup>7</sup>C. M. Lieber and X. Duan, *Adv. Mater.* **12**, 4 (2000).
- <sup>8</sup>Z. W. Pan, Z. R. Dai, and Z. L. Wang, *Science* **291**, 1947 (2001).
- <sup>9</sup>C. Ma, D. Moore, J. Li, and Z. L. Wang, *Adv. Mater.* (in press).
- <sup>10</sup>M. S. Arnold, Ph. Avouris, Z. W. Pan, and Z. L. Wang, *J. Phys. Chem. B* (in press).
- <sup>11</sup>E. Comini, G. Faglia, G. Sberveglieri, Z. Pan, and Z. L. Wang, *Appl. Phys. Lett.* **81**, 1869 (2002).
- <sup>12</sup>V. J. Morris, A. R. Kirby, and A. P. Gunning, *Atomic Force Microscopy for Biologist* (Imperial College Press, London, 1999).
- <sup>13</sup>G. Y. Chen, T. Thundat, E. A. Wachter, and R. A. Warmack, *J. Appl. Phys.* **77**, 3618 (1995).
- <sup>14</sup>J. Fritz, M. K. Baller, H. P. Lang, H. Rothuizen, P. Vettiger, E. Meyer, H. J. Guntherodt, Ch. Gerber, and J. K Gimzewski, *Science* **288**, 316 (2000).
- <sup>15</sup>G. Wu, H. Ji, K. Hansen, Th. Thundat, R. Datar, R. Cote, M. F. Hagan, A. K. Chakraborty, and A. Majumdar, *PNAS* **98**, 1560, (2001).
- <sup>16</sup>X. D. Bai, E. G. Wang, P. X. Gao, and Z. L. Wang, *Appl. Phys. Lett.* (submitted).
- <sup>17</sup>Z. L. Wang and W. L. Hughes, Patent pending, Georgia Tech., 2002.